Journal of Ultrafine Grained and Nanostructured Materials
Vol.48, No.1, June 2015, pp.5-10

Synthesis of nano-sized ceria (CeO_2) particles via a cerium hydroxy carbonate precursor and the effect of reaction temperature on particle morphology

Majid Farahmandjou* and Mahsa Zarinkamar

Department of Physics, Varamin Pishva Branch, Islamis Azad University, Varamin, Iran

Received: 20 December 2014 ; Accepted: 19 May 2015
* *Corresponding author Email: farahamndjou@iauvaramin.ac.ir*

Abstract
Cerium oxide (CeO_2) or ceria has been shown to be an interesting support material for noble metals in catalysts designed for emission control, mainly due to its oxygen storage capacity. Ceria nanoparticles were prepared by precipitation method. The precursor materials used in this research were cerium nitrate hexahydrate (as a basic material), potassium carbonate and potassium hydroxide (as precipitants). The morphological properties were characterized by high resolution transmission electron microscopy (HRTEM), scanning electron microscopy (SEM) and X-ray diffraction (XRD), Fourier transform infrared spectroscopy (FTIR) and UV-Vis spectrophotometer. XRD results showed face centered cubic CeO_2 nanoparticles for annealed nanoparticles at 1000°C. SEM measurement showed that by increasing the calcinations temperature from 200 to 600°C, the crystallite size decreased from 90 to 28 nm. The SEM results showed that the size of the CeO_2 nanoparticles decreased with increasing temperature. The particle size of CeO_2 was around 25 nm as estimated by XRD technique and direct HRTEM observation. SEM and TEM studies showed that the morphology of the prepared powder was sphere-like with a narrow size distribution. The sharp peaks in FTIR spectrum determined the purity of CeO_2 nanoparticles and absorbance peak of UV-Vis spectrum showed the small band gap energy of 3.26 ev.

Keywords: *CeO_2 nanoparticles, cerium (III) nitrate, precipitation, structure properties.*

1. Introduction

Cerium oxide or ceria (CeO_2) have enormous applications in catalysts/catalyst supports [1-2], oxygen ion conductors in solid oxide fuel cells [3-5], electrochemical oxygen pumps [6], UV absorbents [7], fluorescent materials [8] and amperometric oxygen ion monitors because of its high oxygen ion conductivity [9]. CeO_2 nanoparticles have been prepared by sol-gel processing [10-11], sonochemical synthesis [12], a thermal decomposition process [13], hydrothermal synthesis [14], a polymeric precursor route [15], etc. In many of the above processes, the main objective is the synthesis of pure CeO_2 phase based materials for various applications. To obtain high quality nano-sized CeO_2 supports, one of the simple approaches is

the thermal decomposition of a molecular precursor like cerium hydroxycarbonate (CHC: $Ce(OH)CO_3$) at low temperature in air [16, 20]. Several strategies have been proposed for the synthesis of CHC by a chemical precipitation reaction employing an aqueous solution containing cerium (III) nitrate ($Ce(NO_3)_3.6H_2O$) with excess urea [17-21], or ammonium carbonate [18,22] as precipitants. It has also been reported that the bubbling of CO_2 is necessary while precipitating CHC [23]. Ceria (CeO_2) is a cubic fluorite-type structured ceramic material that does not show any known crystallographic change from room temperature up to its melting point (2700°C) [24]. Most of the applications require the use of non-agglomerated nanoparticles, as aggregated nanoparticles lead to inhomogeneous mixing and poor sinter ability. In this article, CeO_2 nanoparticles were prepared via a simple precipitation route. The novelty in this article is that the samples' powders were prepared without washing and purification was done before calcinations resulting in high homogeneity of the samples surface and increasing calcination temperature. The synthesis of CeO_2 nanoparticles requires the use of $Ce(NO_3)_3.6H_2O$ as precursor and potassium hydroxide and potassium carbonate as precipitants. Finally, they were calcined at different temperatures of 600^0C and 1000°C. The surface studies and structural properties of CeO_2 were studied by XRD, HRTEM, and SEM analyses.

2. Materials and Methods

CeO_2 nanoparticles were synthesized by a simple approach according to the following manner. Twenty (20) milliliters each, of potassium hydroxide (0.02 M) and potassium carbonate (0.03 M) were mixed in distilled water by stirring. Then, 40 mL cerium (III) nitrate ($Ce(NO_3)_3.6H_2O$) (0.03 M) was added drop by drop to the solution. The pH decreased from 11 to 6 when the cerium precursor was added. The solution of $Ce(OH)CO_3$ was precipitated while the synthesis temperature increased to 55°C. The resulting CHC were dried at 65°C and cooled to room temperature. Then, the product was aged at 220°C for 2 h. Finally, the product was calcined at 600°C for 3 h to obtain CeO_2 nanopowder.

The specification of the size, structure and morphological properties of the as-synthesis and annealed CeO_2 nanoparticles were carried out. X-ray diffraction (XRD) was used to identify the crystalline phase and to estimate the crystalline size. The XRD patterns were recorded with 2θ in the range of 4-85° with type X-Pert Pro MPD, Cu-K_α: λ = 1.54 Å. The morphology was characterized by scanning electron microscopy (SEM) with type KYKY-EM3200, 25 kV and high resolution transmission electron microscopy (HRTEM) with type Zeiss EM-900, 80 kV. All the measurements were carried out at room temperature.

3. Results and Discussion

The XRD pattern of the samples were carried out to identify crystalline phases and to estimate the crystalline sizes. Figure 1 shows the XRD morphology of CeO_2 nanoparticles calcined at 1000°C for 3 h. The exhibited picks correspond to the (111), (200), (220), (311), (222), (400), (331) and (420) of a cubic fluorite structure of CeO_2 identified using the standard data [22,23]. The mean size of the ordered CeO_2 nanoparticles was estimated from the full width at half maximum (FWHM) and Debye-Sherrer formula, according to equation (1):

$$D = \frac{0.89\lambda}{B\cos\theta} \tag{1}$$

where, 0.89 is the shape factor, λ is the x-ray wavelength, B is the line broadening at half the maximum intensity (FWHM) in radians, and θ is the Bragg angle. The mean size of as-prepared CeO_2 nanoparticles was around 25 nm from this Debye-Sherrer Equation.

From the SEM and HRTEM images of CeO_2 nanoparticles, the morphology of nanoparticles was observed to be nearly spherical with slight agglomeration. Figure 2 shows the SEM images of CeO_2 nanoparticles. In Figure 2(a), to prepare CeO_2 nanoparticles the synthesis temperature was applied and increased to 55°C. It can be seen that the size of CeO_2 increased with increase in synthesis temperature to around 80 nm. In Figure 2(b), the size of nanoparticles decreased with increase in calcination temperature to 600°C for 3 h with slight agglomeration. In Figure 2(c), the CeO_2 nanoparticles were prepared at room temperature. As seen, the size of nanoparticles

decreased when compared to the samples prepared in the presence of synthesis temperature with slight agglomeration. The spherically shaped CeO_2 nanoparticles with clumped distributions are visible through the SEM image (Fig. 2d) when the samples were calcined at 600°C for 3 h. The average crystallite size of calcined nanocrystals is about 25 nm.

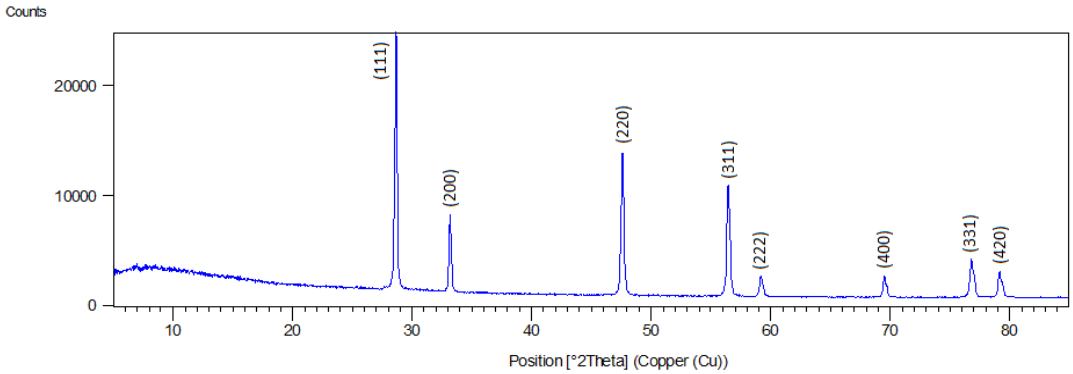

Fig. 1. XRD pattern of Ceo_2 nanoparticles calcined at 1000°C for 3 h

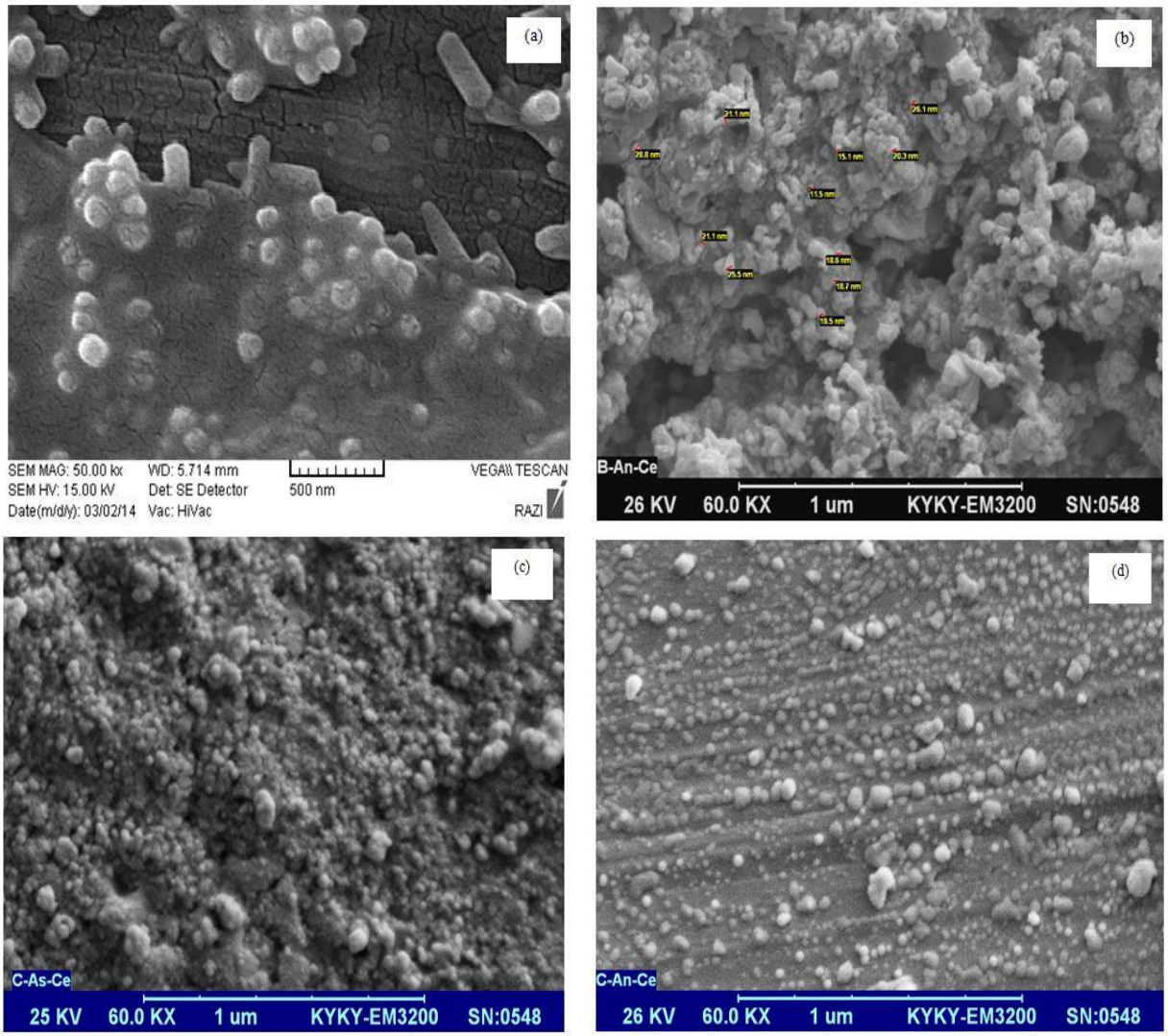

Fig. 2. SEM images of the CeO_2 nanoparticles: (a): synthesized at 55°C, (b): calcined at 600°C, (c): synthesized at room temperature, and (d): calcined at 600°C

The TEM image of as-prepared CeO_2 nanoparticles can be seen in Figure 3. CeO_2 particles are spherical in the size range of 20-80 nm, and aggregate to form clusters.

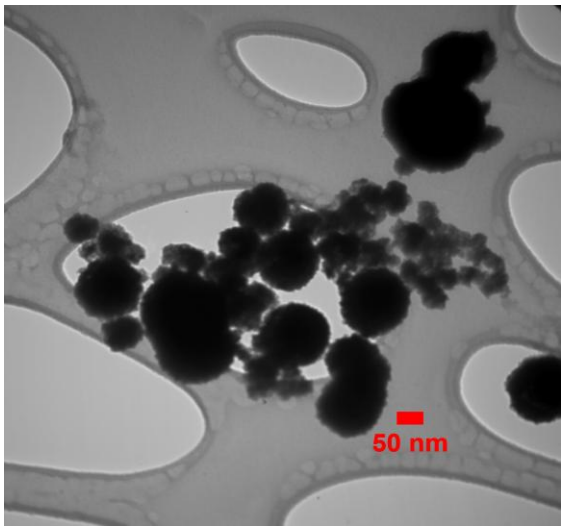

Fig. 3. TEM images of the as-prepared CeO_2 nanoparticles

According to Figure 4, the infrared spectrum (FTIR) of the synthesized CeO_2 nanoparticles was in the range of 400-4000 cm^{-1} wave number and identifies the chemical bonds, as well as functional groups in the compound. The large broad band at 3415 cm^{-1} is ascribed to the O-H stretching vibration in OH^- groups. The absorption peaks around 1464 cm^{-1} were assigned to the bending vibration of C-H stretching. The strong band below 700 cm^{-1} was assigned to the Ce-O stretching mode [24]. The broad band, corresponding to the Ce-O stretching mode of CeO_2 is seen at 500 cm^{-1}.

UV-visible absorption spectral study may assist in understanding the electronic structure of the optical band gap of the material. Absorption in the near ultraviolet region arises from electronic transitions associated within the sample. The UV–Vis absorption spectra of as-prepared and calcined CeO_2 nanoparticles are shown in Figure 5. For as-synthesized CeO_2 nanoparticles, the strong absorption band at low wavelengths near 380 nm corresponds to a band gap energy of 3.26 ev (Fig. 5a) and for calcined CeO_2 nanoparticles, the strong absorption band at low wavelength near 385 nm corresponds to 3.22 ev (Fig. 5b). In comparison with UV-visible absorption spectrum of CeO_2 nanoparticles, band/peak in the spectrum located at around 400-700 nm were observed to be shifted towards the lower wavelength side, which clearly shows the blue shift. It indicates that the absorption positions depend on the morphologies and sizes of CeO_2. The UV absorption ability of CeO_2 is related with band gap energy. The UV-absorption edge provides a reliable estimate of the band gap of any system.

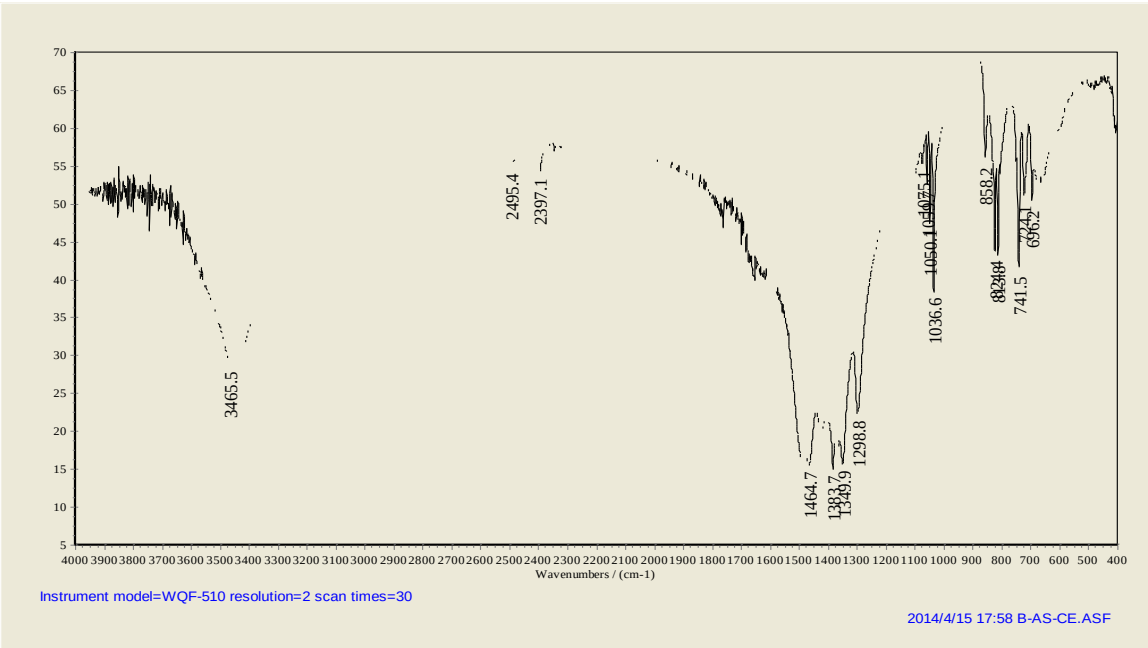

Fig. 4. FTIR spectrum of CeO_2 sample

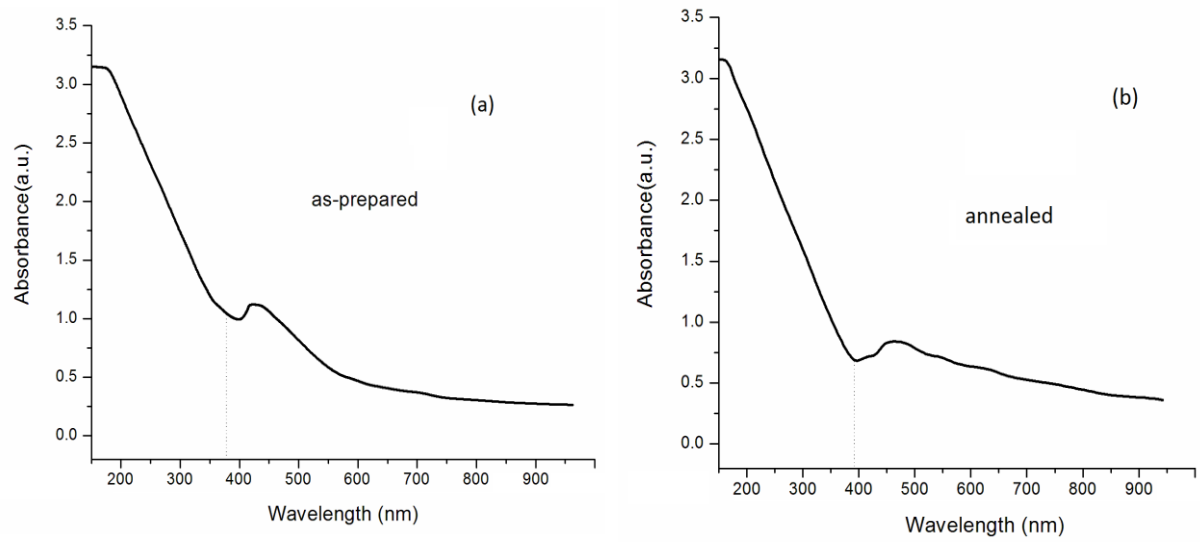

Fig. 5. UV–Vis absorption spectra of CeO_2 nanoparticles: (a): as-synthesized and (b): calcined

4. Conclusion

A simple precipitation technique has been established for the preparation of CeO_2 nanoparticles. The cubic fluorite structure of CeO_2 was identified by XRD, using standard data. From SEM images, it is clear that with increasing synthesis temperature the size of particles increased and nanopowders were less agglomerated. Also, with increasing calcination temperature, the morphology of the particles changed into a spherical shape. The TEM image shows that the as-synthesized spherical CeO_2 nanoparticles prepared by precipitation route, have a diameter in the range of 20-80 nm. From the FTIR data, the presence of Ce-O stretching mode of CeO_2 is shown. The Ceria nanoparticles show a strong UV–vis absorption below 400 nm with a well-defined absorption peak at 380 nm and the direct band gap was found to be 3.26 eV. The shift of the band gap absorption in the UV–vis spectrum agrees closely with the blue shift.

Acknowledgments

The authors are thankful to the Varamin Pishva branch of Islamic Azad University, for the financial support, as well as for the analysis and discussion of results.

References

[1]. J. Zhou, L. Zhao, Q. Huang, R. Zhou and X. Li, Catalytic Activity of Y Zeolite Supported CeO2 Catalysts for Deep Oxidation of 1, 2-Dichloroethane (DCE), Cat. Lett. 127 (2009) 277-284.

[2]. X. Zheng, X. Zhang, S. Wang, X.Wang and S. Wu, Effect of Addition of Base on Ceria and Reactivity of CuO/CeO_2 Catalysts for Low-Temperature CO Oxidation, J. Natural Gas Chem. 16 (2007) 179-185.

[3]. B. Zhu, X. Liu, M. Sun, S. Joi and J. Sun, Calcium doped ceria based materials for Cost effective intermediate temperature solid oxide fuel cells Sun, Solid State Sciences, 5 (2003) 1127-1134.

[4]. T.S. Zhang, J. Ma, L.B. Kong, S.H. Chan and J.A. Kilner, Aging behavior and ... ceramics: a comparative study, Solid State Ionics, 170 (2004) 209-217.

[5]. A. Samson Nesaraj, I. Arul Raj and R. Pattabiraman, Synthesis and characterization of LaCoO based cathode and its chemical compatibility with CeO based electrolytes for intermediate temperature solid oxide fuel cell (ITSOFC), Ind. J. Chem. Tech. 14 (2007) 154-160.

[6]. T. Hibino, K. Ushiki and Y. Kuwahara, Electrochemical oxygen pump using CeO_2 -based solid electrolyte for NOx detection independent of O_2 concentration, Solid State Ionics, 93 (1997) 309-316.

[7]. J.F. de Lima, R.F. Martins, C.R. Neri and O.A. Serra, ZnO: CeO_2 -based nanopowders with low catalytic activity as UV absorbers, App. Surf. Sci. 255 (2009) 9006-9009.

[8]. Y.M. Zhang, M. Hida, H. Hashimoto, Z.P. Luo and S.X. Wang, Effect of rare-earth oxide. (CeO_2) on the microstructures in laser melted layer, J. Mater. Sci. 35 (2004) 5389-5400.

[9]. A.K. Sinha and K. Suzuki, Preparation and characterization of novel mesoporous ceria-titania, J. Phy. Chem. B, 109 (2005) 1708-1714.

[10]. K. Jiang, J. Meng, Z. He, Y. Ren and Q. Su, Sol-gel synthesis and electrical properties of ceria-based solid electrolytes, Sci. in China Series B: Chem. 42 (1999) 159-163.

[11]. L.L. Shaw, C. Shen and E.L. Thomas, Synthesis of gadolinia-doped ceria gels and powders from acetylacetonate precursors, J. Sol-Gel Sci. Tech. 53 (2010) 1-11.

[12]. J. Guo, X. Xin, X. Zhang, S. Zhang, Ultrasonic-induced synthesis of high surface area colloids CeO_2 – ZrO_2, J. Nanoparticle Res. 11 (2009) 737-741.

[13]. M. Kamruddin, P.K. Ajikumar, R. Nithya, A.K. Tyagi and B. Raj, Synthesis of nanocrystalline ceria by thermal decomposition and soft-chemistry methods, Scripta Materialia, 50 (2004) 417-422.

[14]. A.I.Y. Tok, F.Y.C. Boey, Z. Dong and X.L. Sun, Hydrothermal synthesis of CeO_2 nanoparticles, J. Mater. Processing Tech. 190 (2007) 217-222.

[15]. A. Valentini, N.L.V. Carreno, L.F.D. Probst, A. Barison, A.G. Ferreira, E.R. Leite and E. Longo, Ni: CeO_2 nanocomposite catalysts prepared by polymeric precursor method, Appl. Cataly. A: General, 310 (2006) 174-182.

[16]. J.G. Li, T. Ikegami, Y. Wang, T. Mori, Review of fuel processing catalysts for hydrogen production in PEM fuel cell systems, (2002) J Am Ceram Soc 85:2376.

[17]. J. Bai, Z. Xu, Y. Zheng, H. Yin, Shape control of CeO_2 nanostructure materials in microemulsion systems, (2006) Mater Lett 60:1287.

[18]. Z. Guo, F. Du, Z. Cui, Synthesis and characterization of bundle-like structures consisting of single crystal $Ce(OH)CO_3$ nanorods, (2007) Mater Lett 61:694 .

[19]. B. Ksapabutr, E. Gulari, S. Wongkasemjit, Sol–gel derived porous ceria powders using cerium glycolate complex as precursor, (2006) Mater Chem Phys 99:318.

[20]. J.P. Viricelle, M. Pijolat, M. Soustelle, C. Zing, Transformation of cerium(III) hydroxycarbonate into ceria, (1995) J Chem Soc Faraday Trans 91:4431.

[21]. D. Zhang, W. Wu, X. Ni, X. Cao, X. Zhang, X. Xu, S. Li, G. Han, A. Ying, Z. Tong, Fabrication and characterization of novel bowknot-like CeO2 crystallites and applications for Methyl-orange Sensors, (2009) J Mater Sci 44:3344 ,

[22]. M.Y. Cho, K.C. Roh, S.M. Park, H.J. Choi, J.W. Lee, Control of particle size and shape of precursors for ceria using ammonium carbonate as a precipitant, (2010) Mater Lett 64:323.

[23]. K. Foger, M. Hoang, T.W. Turney, Formation and thermal decomposition of rare-earth carbonates, (1992) J Mater Sci 27:77.

[24]. K. Reinhardt, H. Winkler. (2002) Cerium mischmetal, cerium alloys, and cerium compounds. In: Ullmann's encyclopedia of industrial chemistry. Vol. 7. Weinheim, Germany: Wiley-VCH, pp. 285–300.